Markedly perturbed hematopoiesis in acid ceramidase deficient mice

Acid ceramidase (ACDase) is ubiquitous and catalyzes the degradation of ceramide. ACDase and ceramides have been implicated in many disorders, including cancer, obesity, diabetes, inflammation, and neurodegenerative diseases.[1-3] Deficiencies in ACDase activity lead to Farber disease, but the specific role of this reaction in hematopoiesis has not been clarified. We previously reported that *Asah1*$^{P361R/P361R}$ mice have enlarged hematopoietic organs with leukocytosis, specifically neutrophilia and monocytosis, along with an excess of macrophages.[4] Here we establish that the organ enlargement is due to a gradual accumulation of foamy macrophages, which destroys the tissue architecture. Lymphoid progenitors in the bone marrow (BM) and thymus of *Asah1*$^{P361R/P361R}$ mice were severely reduced over time and myeloid progenitors were increased. Both progenitor populations were not intrinsically altered by ceramide accumulation and, importantly, were able to reconstitute a wild-type (WT) mouse without inducing Farber disease.

Due to the rarity of patients diagnosed with Farber disease and their shortened lifespan, hematopoietic defects have only been described superficially. Case reports have mentioned some hematologic manifestations, but presentation has been inconsistent. These manifestations include hepatosplenomegaly, enlargement and calcification of axillary lymph nodes (LN), peripheral blood leukocytosis, anemia, thrombocytopenia, and occasional nucleated RBCs.[5-8] Most Farber patients present with subcutaneous nodules that may contain foamy histiocytes.[5-9]

Our first aim was to determine the cause of hematopoietic organ enlargement in our murine model of ACDase deficiency. Surprisingly, the 3-12 fold enlargement of the hematopoietic organs was not due to an increase in total recoverable cells (Table 1). The cell number in the BM, spleen, and thymus was actually reduced by 40%-85%, and there was no significant difference in the cell number in the LN. This decline in cell number occurs precipitously between weeks 5 and 9, near the end of the lifespan of the animal (*data not shown*). Instead, the hematopoietic organ enlargement was due to foamy macrophages. An increase of large, unstained (pale) areas could be detected in 9-week old *Asah1*$^{P361R/P361R}$ animals in H&E stained sections (Figure 1A). These areas were B220$^-$ CD3$^-$ Mac-2$^+$, suggesting cells of the myeloid lineage. These Mac-2$^+$ cells were much larger in size than lymphocytes or Mac-2$^+$ macrophages in WT BM and were consistent with foamy macrophages described in other LSDs.[10,11] However, they were not "sea blue" after May-Grunwald and Giemsa staining, as described in Niemann-Pick disease.[12] These macrophages were also F4-80$^-$ CD23$^-$, and could bind IgM (*data not shown*). From 5-9 weeks such foamy macrophages increased in size and numbers (*data not shown*). Histiocytic infiltrations have been found in biopsies of the liver, spleen, BM, lungs, thymus, LN, heart, spine, and peritoneal fluid of Farber patients.[6,9,13,14] Furthermore, the age of onset of dermal nodules (filled with histiocytes) has been suggested to correlate with life expectancy.[15] Antonarakis *et al*. describe a patient with normal peripheral blood (PB) counts initially that rapidly succumbed to the disorder as the PB counts increased; post-mortem analysis revealed massive histiocytic infiltration in organs.[6]

Table 1. Weights and total cells isolated from WT, Het, and Hom *Asah1*$^{P361R/P361R}$, and BMT mouse organs.

Measurement	WT (unit ± SEM)	Het (unit ± SEM)	Hom (unit ± SEM)	BMT, (unit ± SEM)	Fold difference, Hom/WT	Fold difference, BMT/Hom	Fold difference, BMT/WT
Body weight (g)	28.36±1.21	26.43±1.05	11.87±0.29	30.82±2.97	0.419x ***	2.60x ***	1.09x N.S
Spleen % weight	0.29%±0.02%	0.29%±0.03%	1.2% ± 0.1%	0.92%±0.68%	4.10x ***	0.0621x N.S.	3.15x N.S.
Thymus % weight	0.27%±0.02%	0.29%±0.02%	0.78% ± 0.12%	0.17%	3.00x ***	0.0101x N.D.	0.64x N.D.
Lymph node % weight	0.0089%±0.0020%	0.013%±0.001%	0.11%±0.01%	0.0049%±0.0008%	12.2x ***	0.0003x ***	0.56x N.S.
Liver % weight	5.4%±0.3%	5.3%±0.4%	7.4%±0.5%	4.9%±0.7%	1.37x **	0.3774x *	0.91x N.S.
Kidney % weight	0.81%±0.08%	0.90%±0.11%	1.0%±0.1%	0.81%±0.08%	1.27x N.S.	0.0582x N.S.	0.99x N.S
Total bone marrow cells per leg	4.17E7±0.55E7	N.D.	2.44E7±0.28E7	1.22E8±2.15E7	0.585x **	5.0x ***	3x ***
Total spleen cells	1.17E8±0.26E8	N.D.	3.75E7±0.99E7	2.06E9±1.64E9	0.321x **	55x *	17x *
Total thymus cells	8.96E7±0.53E7	N.D.	1.42E7±0.63E7 0.63E7	4.2E8	0.158x ***	30x N.D.	5x N.D.
Total lymph node cells	2.56E6±0.41E6	N.D.	4.01E6±1.93E6	N.D.	1.57x N.S.	N.D.	N.D.

WT, Het, and Hom Asah1$^{P361R/P361R}$ *mice were weighed at age nine weeks. BMT mice were weighed at six months following control mice transplanted with age-matched Asah1*$^{P361R/P361R}$ *donor cells. Body weight is expressed in grams (n=11-13 for WT, Het, Hom; n=4 for BMT). Organ values are expressed as percent of body weight (n=4-9 per group). Lymph node weight was calculated by averaging 2-4 proper axillary and accessory axillary lymph nodes. Total cells were counted from bone marrow and spleen (n=15-16 for WT, Het, Hom; n=4 for BMT) and from lymph nodes and thymus (n=4 per group, except for thymus BMT where n=1 (thymuses could not be seen in the other 3 mice)). Significance for an unpaired, two-tailed t-test is listed under each fold difference. N.S.: nonsignificant; N.D.: not determined.*

The macrophage infiltration into tissues was so severe in our model that the architecture of the organs was altered. While WT thymuses showed distinctive cortex and medulla, no such architecture could be detected in sections from *Asah1*$^{P361R/P361R}$ mice after five weeks of age (Figure 1A). Flow cytometry analyses revealed a time-dependent and precipitous decline of the CD4$^+$ CD8$^+$ T cell populations in the thymuses of *Asah1*$^{P361R/P361R}$ mice from more than 77% in WT mice to less than 9% in *Asah1*$^{P361R/P361R}$ mice by nine weeks, with a similar decline in absolute cell numbers (Figure 1B and C) that correlated with disease progression (Figure 1D). A similar progenitor cell decline was seen in the BM where flow cytometry analyses revealed a decline of B cell progenitor populations in *Asah1*$^{P361R/P361R}$ mice, both in population

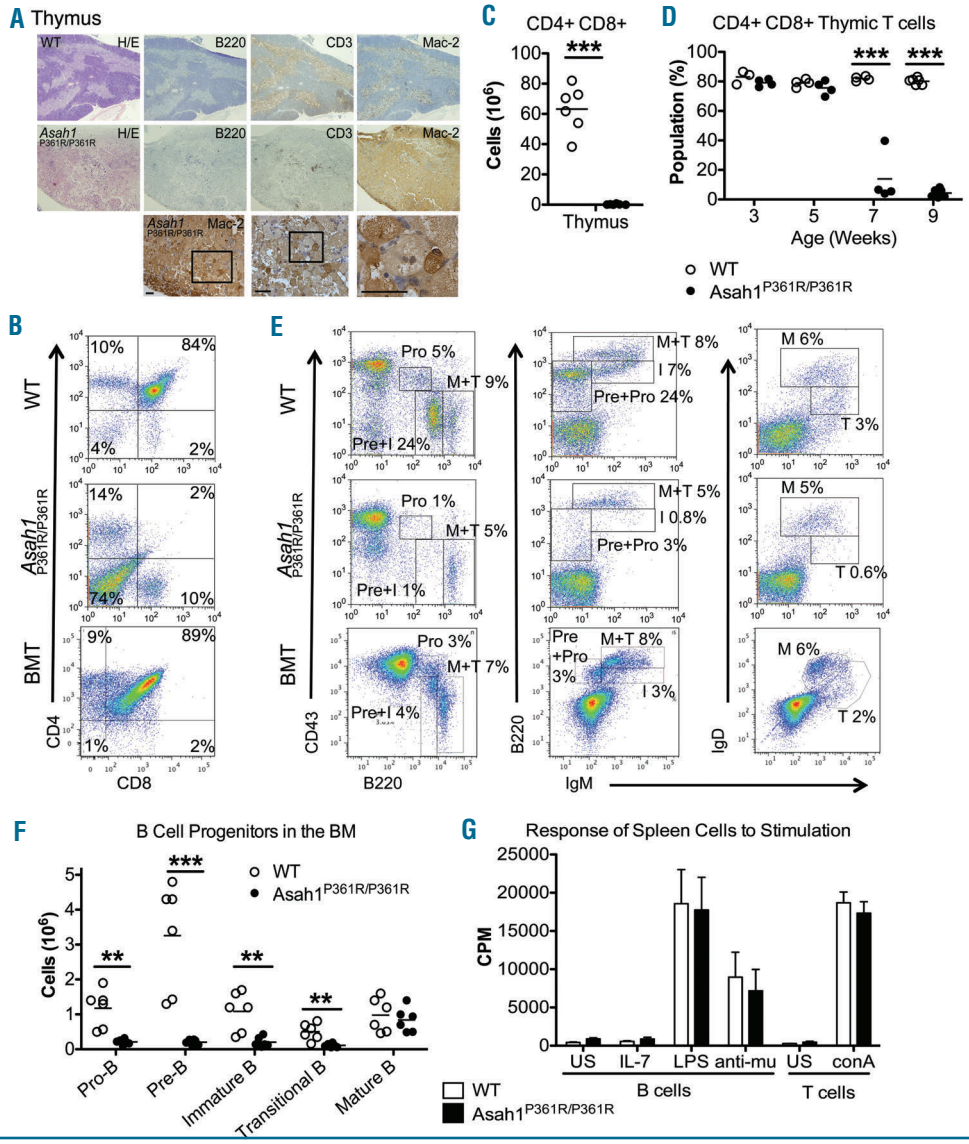

Figure 1. *Asah1*$^{P361R/P361R}$ mouse hematopoietic organs are filled with foamy macrophages, and have reduced but functional B and T cell progenitors. (A) Staining of the thymuses of WT (top row) and *Asah1*$^{P361R/P361R}$ mice (middle row) at nine weeks with hematoxylin and eosin (H&E), B220, CD3, and Mac-2 revealed fewer B220$^+$ and CD3$^+$ cells, and instead a massive increase of large, Mac-2$^+$ cells reminiscent of foamy macrophages. Destroyed cortex/medulla architecture of the thymus is seen. A similar accumulation of Mac-2$^+$ cells and destruction of architecture were seen in the BM, spleen, and lymph nodes. Foamy macrophages are severely enlarged (bottom row; consecutive panels are a close up of boxed area) Scale bar 50 μm. (B) Flow cytometry analysis was performed on thymuses from 9-week old WT and *Asah1*$^{P361R/P361R}$ thymuses following staining for T cell markers. CD4$^+$ CD8$^+$ T cells comprise approximately 80% of the thymus in WT mice, yet are almost absent in *Asah1*$^{P361R/P361R}$ mice. This population was present in BMT mice (control mice receiving *Asah1*$^{P361R/P361R}$ bone marrow). (C) The reduction in cell population percentage is also seen when presented as absolute cell numbers. Significance was assessed using an unpaired, two-tailed *t*-test. (D) CD4$^+$ CD8$^+$ cells are present in normal numbers in *Asah1*$^{P361R/P361R}$ mice at three and five weeks; a drastic decline is seen at seven and nine weeks. Significance was assessed using a one-way ANOVA with Bonferroni post test. Data represent individual mice; line represents the mean. (E) Flow cytometry analysis was performed on BM from 9-week old WT and *Asah1*$^{P361R/P361R}$ mice following staining for B-lineage markers. B cell progenitors constituted a smaller percentage of total BM in *Asah1*$^{P361R/P361R}$ mice. This includes pro-B cell, pre-B cell, immature B cell, and transitional B cells. In contrast, mature B cells were present at a normal percentage in the BM. (F) The absolute number of B cell progenitors at each progenitor stage were depleted, while mature B cells were maintained. Significance was assessed using an unpaired, two-tailed t-test for each cell type. Data represent individual mice; line represents the mean. Pro: pro-B cell; Pre: pre-B cell; I: immature B cell; T: transitional B cell; M: mature B cell. (G) To assess the functionality of mature lymphoid cells, spleen cells from 9-week old WT and *Asah1*$^{P361R/P361R}$ were stained for CD19 to select for B cells. Their response to IL-7, LPS, and anti-mu *in vitro* was similar. Spleen cells selected for CD3 (T cells) were tested for their response to conA and their response was also similar. n=4 per genotype for IL-7, LPS, and anti-mu. n=2 for conA. Experiment performed twice. US: unstimulated; LPS: lipopolysaccharide; conA: concanavalin A.

percentages and absolute cell numbers at nine weeks (Figure 1E and F). As in the thymus, the decline began at 5-7 weeks of age, but in contrast, the quantity of mature B cells was not affected. The missing T and B progenitors were not found in the PB (*data not shown*). The coincidental timing of the increase in macrophage infiltration into the thymus and BM with the reduction in T- and B-progenitor cells, respectively, suggests that destruction of the architecture by macrophages may be disrupting the niche for developing cells.

Despite the absence of B and T cell progenitors in the BM and thymus of *Asah1*$^{P361R/P361R}$ mice, respectively, mature B and T cells were found in the circulation and organs. These mature cells were able to respond to stimulation *in vitro* in lymphocyte proliferation assays (Figure 1G). This demonstrates that the mature B and T cells from this model maintain functionality. The presence of mature B and T cells at an age where B and T progenitors are almost completely depleted suggests that these cells were produced earlier in the mouse's life when B and T cell progenitors were present and the environment was able to support differentiation. Either the B and T progenitors lost their ability to differentiate or the environment lost its ability to support them. Arguing against the former explanation, the functionality of the progenitor cells from *Asah1*$^{P361R/P361R}$ mice, as assessed *in vitro*, appeared unaffected. B-cell progenitors from 9-week old mice maintained the capacity to respond to IL-7 stimulation *in vitro* (*data not shown*). Similarly, myeloid cells were able to differentiate into all lineage types in *in vitro* colony-forming cell (CFC) assays (Figure 2A). The CFC results indicate that the monocytosis reported in the PB of *Asah1*$^{P361R/P361R}$ mice[4] and the foamy macrophages found in their organs is not due to a disproportionate increase of monocyte progenitor cells (CFU-M or CFU-GM) in the BM. Similarly, we previously reported that *Asah1*$^{P361R/P361R}$ mice have an excess of RBCs,[4] but it is not from a disproportionate increase of BFU-

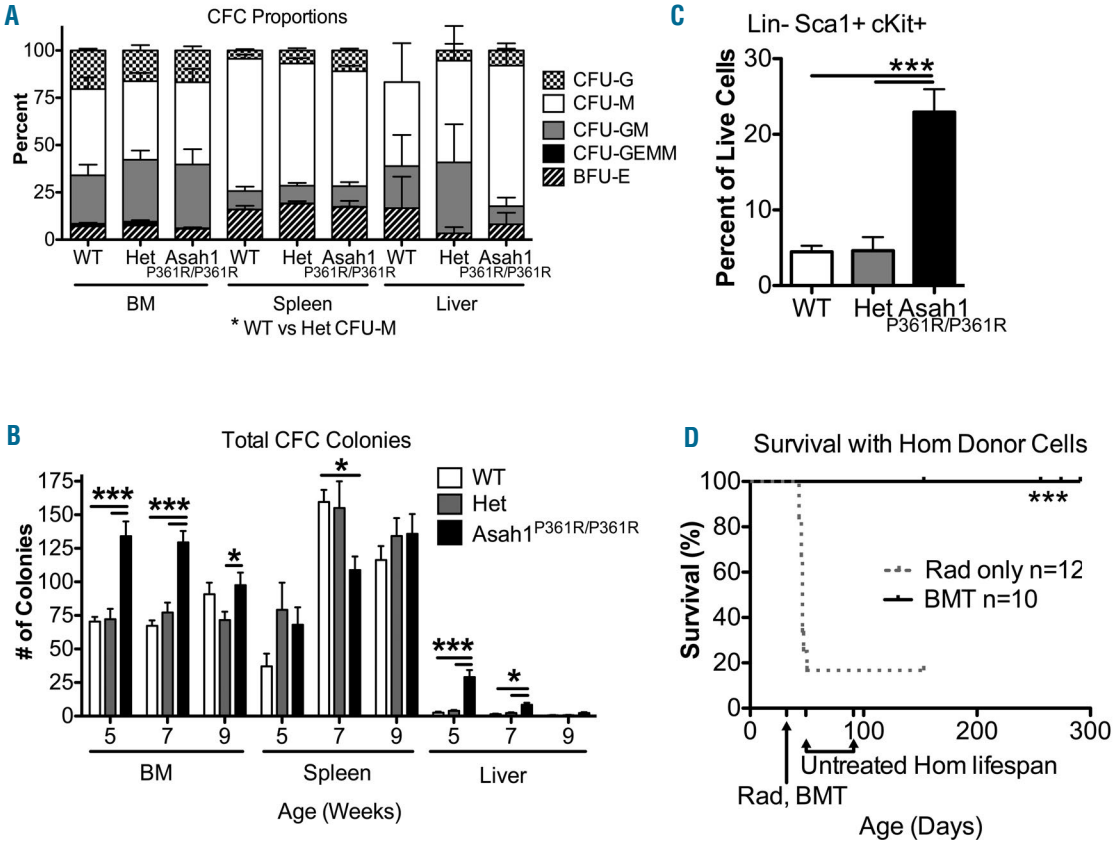

Figure 2. Myeloid progenitors are not intrinsically altered in *Asah1*$^{P361R/P361R}$ mice, and *Asah1*$^{P361R/P361R}$ BM is able to rescue lethally irradiated control mice and is not sufficient to induce Farber disease. (A) Myeloid cells were assessed by CFC assay. Colony types were scored by visual examination. The differentiation ability of the progenitors in the BM, spleen, and liver of *Asah1*$^{P361R/P361R}$ mice were not significantly different from WT and Het mice. Significance was assessed by a two-way ANOVA with Bonferroni post test. (B) More myeloid progenitors are present in the BM of *Asah1*$^{P361R/P361R}$ mice compared to WT and Het mice at all ages. In the spleen, fewer colonies were in the spleen of *Asah1*$^{P361R/P361R}$ mice at seven weeks compared to WT mice. In the liver, an increase in myeloid progenitors was seen at five weeks, which declined over time. CFU-Meg were rare in the CFC of both WT and *Asah1*$^{P361R/P361R}$ assays and were not included in the counts. Significance was assessed by a two-way ANOVA with Bonferroni post test. n=6-7 per genotype per week for CFC assays. CFU: colony forming unit; G: granulocyte; M: monocyte; GM: granulocyte/monocyte; GEMM: granulocyte/monocyte/megakaryocyte/erythrocyte; BFU-E: burst forming unit erythrocyte. (C) BM from 9-week old mice was stained for lineage markers, Sca1 and cKit (LSK) to identify HSPC. An increase in the percentage of LSK cells was seen in BM from *Asah1*$^{P361R/P361R}$ mice. A similar increase was seen in the absolute number of LSK cells (*data not shown*). Significance was assessed by a one-way ANOVA with Bonferroni post test. n=8 for WT and *Asah1*$^{P361R/P361R}$; n=3 for Het. (D) BM enriched for HSPC by 5-fluorouracil pre-treatment of donors was transplanted from *Asah1*$^{P361R/P361R}$ mice into lethally irradiated WT mice (BMT). *Asah1*$^{P361R/P361R}$ cells were able to reconstitute the hematopoietic system of the recipients. BMT mice had a lifespan longer than untreated Hom mice (range indicated by arrows). Control mice not receiving a BMT after radiation had a lethality rate of 85%. Significance was assessed by a log rank Mantel-Cox test.

E (Figure 2A). Instead these cells may be from the liver: *Asah1*$^{P361R/P361R}$ livers contained many more myeloid CFCs than control livers at five weeks, with the difference gradually decreasing at seven and nine weeks (Figure 2B). Extramedullary hematopoiesis has been noted in one very severe Farber disease patient that died three days after birth,[9] and would be consistent with emergent granulopoiesis observed during inflammation. Indeed, an accumulation of granulocytes was seen in the thymuses, LNs, and spleens of our *Asah1*$^{P361R/P361R}$ mice, as determined by Mac-1 and Gr-1 staining (*data not shown*).

Interestingly, there was an increase in total myeloid progenitor cell colonies seen in BM from *Asah1*$^{P361R/P361R}$ mice at five, seven, and nine weeks (Figure 2B). The results of the CFC assay were recapitulated by flow analyses of lineage$^-$ Sca1$^+$ cKit$^+$(LSK) cells; Homozygous BM at nine weeks had an increase in LSK cells (Figure 2C). The difference in colony numbers in the CFC assays in samples originating from *Asah1*$^{P361R/P361R}$ mice was smaller at nine weeks compared to five and seven weeks. Spleen myeloid progenitors were decreased in *Asah1*$^{P361R/P361R}$ mice only at seven weeks but, like the BM, the differentiation potential was similar to cells from WT controls (Figure 2A and B).

Together, the presence of mature B and T cells that appear functional, and the assessment of myeloid progenitors by the CFC assay data, suggest that lymphoid and myeloid progenitor cells themselves are not negatively affected by ACDase deficiency. Instead, we hypothesize that there is a degeneration of the niche that can no longer support these lineages. To support this hypothesis, we tested the ability of the myeloid and lymphoid cells to differentiate in a normal environment *in vivo* by transplanting *Asah1*$^{P361R/P361R}$ donor cells into WT and Het mice. The *Asah1*$^{P361R/P361R}$ donor cells (BMT) were able to reconstitute hematopoiesis in this normal environment at 60%-100% donor chimerism at eight months post transplant, as measured by CFC assay with and without G418, and PCR of these colonies. Infusion of the *Asah1*$^{P361R/P361R}$ donor cells did not result in the WT recipient mice developing signs of Farber disease. The mice survived past the lifespan of Farber mice (Figure 2D), maintained a normal body weight (Table 1), and did not develop leukocytosis (*data not shown*). The spleen, LN, liver, and thymus sizes were reduced to normal WT sizes (Table 1). The total amount of cells recovered from the BM, spleen, and thymus of BMT mice was greater than in control WT or *Asah1*$^{P361R/P361R}$ animals. In addition, these organs were not filled with foamy Mac-2$^+$ macrophages (*data not shown*). The single thymus that was found had a normal proportion of CD4$^+$ CD8$^+$ T cells (Figure 1B). Similarly, B-cell progenitors were present at normal levels (Figure 1E). Together, these data suggest that *Asah1*$^{P361R/P361R}$ hematopoietic cells alone are not sufficient to induce Farber disease in a WT environment. Alternatively, WT tissues transferred low levels of functional ACDase to the donor *Asah1*$^{P361R/P361R}$ cells through mannose-6-phosphate receptor-mediated uptake.

These data show for the first time that systemic ACDase deficiency leads to the generation of an abnormal hematopoietic environment that initiates histiocytosis, which in return leads to the complete destruction of organ architecture. ACDase deficiency does not appear to intrinsically affect the differentiation of hematopoietic progenitor cells, but our data suggest it has a detrimental effect on the developmental niche for hematopoietic cells. Identifying the roles of ACDase and ceramide at important junctures in hematopoiesis is critical for understanding and developing therapies for Farber disease and other disorders in which ceramide accumulates, including inflammation, cancer, obesity, and diabetes.

Shaalee Dworski,[1] Alexandra Berger,[2] Caren Furlonger,[2] Joshua M. Moreau,[3] Makoto Yoshimitsu,[4] Jessa Trentadue,[2] Bryan C.Y. Au,[2] Christopher J. Paige,[2,3,5] and Jeffrey A. Medin[1,2,5]

[1]Institute of Medical Science, University of Toronto, Canada; [2]University Health Network, Toronto, Canada; [3]Department of Immunology, University of Toronto, Canada; [4]Division of Hematology and Immunology, Center for Chronic Viral Diseases, Graduate School of Medical and Dental Sciences, Kagoshima University, Japan; and [5]Department of Medical Biophysics, University of Toronto, Canada

Funding: this work was supported in part by funding from: NIH 1R21NS078191- 01A1 (JAM), Vaincre Les Maladies Lysosomales (VML) (JAM), the Canadian Institutes of Health Research Training Program in Biological Therapeutics Traineeship (SD), and funding from the Princess Margaret Cancer Centre Foundation (AB, CF, JMM, CJP).

Correspondence: jmedin@uhnres.utoronto.ca

doi:10.3324/haematol.2014.108530

Key words: hematopoiesis, acid ceramidase deficient mice, histiocytosis, organ architecture, Farber disease.

Information on authorship, contributions, and financial & other disclosures was provided by the authors and is available with the online version of this article at www.haematologica.org.

References

1. Morad SA, Cabot MC. Ceramide-orchestrated signalling in cancer cells. Nat Rev Cancer. 2013;13(1):51-65.
2. Bikman BT. A role for sphingolipids in the pathophysiology of obesity-induced inflammation. Cell Mol Life Sci. 2012;69(13):2135-2146.
3. Mielke MM, Bandaru VVR, Haughey NJ, et al. Serum ceramides increase the risk of Alzheimer disease: the Women's Health and Aging Study II. Neurology. 2012;79(7):633-641.
4. Alayoubi AM, Wang JCM, Au BCY, et al. Systemic ceramide accumulation leads to severe and varied pathological consequences. EMBO Mol Med. 2013;5(6):827-842.
5. Levade T, Sandhoff K, Schulze H, Medin J. Acid ceramidase deficiency: Farber lipogranulomatosis. Scriver's OMMBID (The Online Metabolic & Molecular Bases of Inherited Disease), Valle, Beaudet, Vogelstein, Kinzler, Antonorakis, and Ballabio, eds. (McGraw-Hill). 2009.
6. Antonarakis SE, Valle D, Moser HW, Moser A, Qualman SJ, Zinkham WH. Phenotypic variability in siblings with Farber disease. J Pediatr. 1984;104(3):406-409.
7. Mondal RK, Nandi M, Datta S, Hira M. Disseminated lipogranulomatosis. Indian Pediatr. 2009;46(2):175-177.
8. Fujiwaki T, Hamanaka S, Koga M, et al. A case of Farber disease. Acta Paediatr Jpn. 1992;34(1):72-79.
9. Kattner E, Schäfer A, Harzer K. Hydrops fetalis: manifestation in lysosomal storage diseases including Farber disease. Eur J Pediatr. 1997;156(4):292-295.
10. Pacheco CD, Lieberman AP. The pathogenesis of Niemann-Pick type C disease: a role for autophagy? Expert Rev Mol Med. 2008;10:e26.
11. Kanzaki S, Yamaguchi A, Yamaguchi K, et al. Thymic alterations in GM2 gangliosidoses model mice. PLoS One. 2010;5(8):e12105.
12. Sharma P, Kar R, Dutta S, Pati HP, Saxena R. Niemann-Pick disease, type B with TRAP-positive storage cells and secondary sea blue histiocytosis. Eur J Histochem. 2009;53(3):183-186.
13. Van Lijnschoten G, Groener JEM, Maas SM, Ben-Yoseph Y, Dingemans KP, Offerhaus GJA. Intrauterine Fetal Death Due to Farber Disease: Case Report. Pediatr Dev Pathol. 2000;3(6):597-602.
14. Jarisch A, Steward CG, Sörensen J, et al. Odontoid infiltration and spinal compression in Farber Disease: reversal by haematopoietic stem cell transplantation. Eur J Pediatr. 2014;173(10):1399:1403.
15. Burck U, Moser H, Goebel H, Grüttner R, Held K. A case of lipogranulomatosis Farber: some clinical and ultrastructural aspects. Eur J Pediatr. 1985;143(3):203-208.